Suppression of IVUS Image Rotation.
A Kinematic Approach

Misael Rosales[1,2], Petia Radeva[2], Oriol Rodriguez[3], and Debora Gil[2]

[1] Lab. de Física Aplicada, Fac. de Cs.
Dpto. de Física (ULA), Mérida/Venezuela
misael@cvc.uab.es
[2] CVC, Edifici O, Campus UAB, 08193 Bellaterra, Spain
[3] Universitary Hospital "Germans Tries i Pujol", Badalona, Spain

Abstract. IntraVascular Ultrasound (IVUS) is an exploratory technique used in interventional procedures that shows cross section images of arteries and provides qualitative information about the causes and severity of the arterial lumen narrowing. Cross section analysis as well as visualization of plaque extension in a vessel segment during the catheter imaging pullback are the technique main advantages. However, IVUS sequence exhibits a periodic rotation artifact that makes difficult the longitudinal lesion inspection and hinders any segmentation algorithm. In this paper we propose a new kinematic method to estimate and remove the image rotation of IVUS images sequences. Results on several IVUS sequences show good results and prompt some of the clinical applications to vessel dynamics study, and relation to vessel pathology.

1 Introduction

The introduction of the IntraVascular UltraSound (IVUS) in the field of medical imaging [1, 2] as an exploratory technique has significantly changed the understanding of the arterial diseases and individual patterns of diseases in coronary arteries. Each IVUS plane visualizes the cross-section (Fig. 1 (left)) of the artery allowing extraction of qualitative information about: the causes and severity of the narrowing of the arterial lumen, distinction of thrombus of the arteriosclerotic plaque, recognition of calcium deposits in the arterial wall, determination and location of morpho-geometrics arteries parameters [3, 4, 5], among others. The main role of IVUS is to serve as a guide in the interventional procedures allowing to measure the morphological structures along the vessel. Artifacts caused by the periodic rotation of the image, introduce an error in the measurements precision in tangential direction [6, 8]. The vessel wall follows a periodic oscillatory motion in an image sequence corresponding to the heart cycles. This motion has a rotation center positioned on the vessel wall border in most cases. We can visually evidence this effect by using the mean of an IVUS sequence along its temporal direction, as shown in Fig. 1 (right). This image represent the average grey level of pixels along 25 frames corresponding to approximately one heart
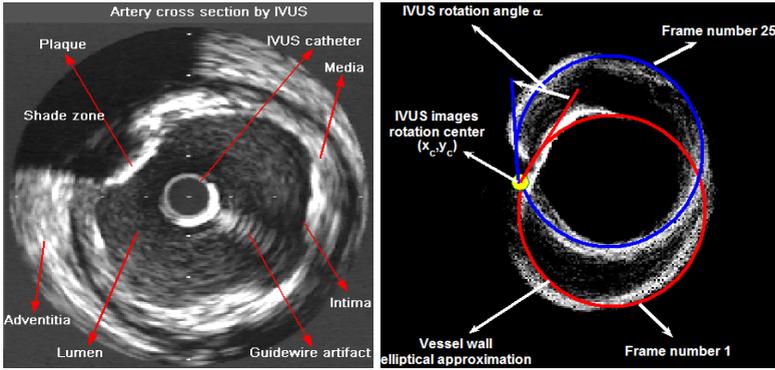
Fig. 1. Morphological arterial structures and artifacts (left). Empirical evidence of IVUS rotation effect (right)

cycle. Since brighter structures correspond to the vessel wall, in this particular case, the center of rotation is the most "brilliant point". The main goal of this work is to estimate and remove the rotation effect, in order to improve the longitudinal IVUS visualization. Instead of using an optical flow scheme, prone to be misled by blood random movement, we suggest using kinematic principles. A good estimation of the rotation images gives the possibility of understanding their mechanical and physiological genesis providing the possibility to study in a robust form the vessel dynamics, and to establish new diagnostic tools. The article is organized as follows: In section 2 we discuss some physical considerations about the rotation effect, the general aspect over the kinematic model is discussed in section 2.1, the neuronal network training procedures are explained in section 2.2 and the estimation and removing procedures of the rotation effect are discussed in sections 2.3 and 2.4, respectively. Finally, the results and conclusions are explained in sections 3 and 4.

2   Physical Considerations of IVUS Image Rotation

The IVUS rotation effect is an image sequence artifact described by various authors [6, 8, 10] as a gray levels shift in the vessel tangential direction, that avoids reliable measurements of distance in longitudinal views. There are two main reasons of this artifact: mechanical and anatomic-physiological factors. The mechanical factor corresponds to the catheter movement during pullback. This motion is locally caused by pulsatile blood flow, the vessel wall dilation and the intrinsic heart muscle dynamics and globally by the catheter trajectory geometry. Anatomic factor is due to the dynamic response of the intrinsic vessel architecture to blood pressure and its mutual interaction with the heart muscle. We model the rotation artifact as follows:

2.1   Kinematic Model for Rotation Estimation

In order to find the rotation center of the sequence, we consider that the vessel wall shape can be modelled as a discrete structure, which temporal evolution depends on the reciprocal interaction between the radial force that comes from the blood pulse and the vessel wall local shape perceived by the catheter. Current IVUS techniques assume that the vessel is circular, the catheter is located in the center of the artery, and the transducer is parallel to the long axis of the vessel. However, both transducer obliquity and vessel curvature can produce an image giving the false impression that the vessel is elliptical. Transducer obliquity is especially important in large vessels and can result in an overestimation of dimensions and reduction of image quality [6]. In general, each image sequence has its own center of rotation. This center can stay at rest or change the spatial position along the sequence. In order to find such center of rotation, we will assume that the vessel wall is a discrete linear elastic oscillating system, with a total energy coming from the pulsatile radial force of the heart blood pulse [11]. Because arterial structures have approximately an elliptical shape, we use polar coordinates to study their temporal evolution. It follows that if the trajectory is given by: $(x, y) = (r(t)cos(\theta(t)), r(t)sin(\theta(t)))$, the total energy of one element (x_i, y_i) of the vessel wall is equal to:

$$E_i = T_i + U_i \tag{1}$$

$$where \quad T_i = \frac{m_i v_i^2}{2} + \frac{m_i}{2}(r_i \omega_i)^2 \quad U_i = \frac{k_i r_i^2}{2}$$
$$v_i = \sqrt{vx_i^2 + vy_i^2} \quad r_i = \sqrt{x_i^2 + y_i^2} \quad w_i = \frac{\partial \theta_i}{\partial t}.$$

The quantities T_i and U_i are the kinetic and elastic energy respectively, m_i, v_i, ω_i and k_i are the mass, tangential velocity, angular velocity and elasticity constant of the i-th element of the vessel wall. In this paper the elastic constant is set to $k_i = 1$. The mass of one element can be estimated considering the minimal "voxel" volume $V_b \approx 6.4 \times 10^{-5} \ mm^3$ swept by the ultrasound beam [14]. Using this fact, the element of mass is $m = \rho * V_b \approx 1.09 \frac{grs}{cm^3} * 6.4 \times 10 - 8grs \approx 6.97 \times 10^{-5} kg$, where ρ is the tissue density [12]. Within the above kinematic framework, the rotation center along the IVUS sequence is represented by the region in the vessel wall that has minimal total energy. The steps to compute and suppress the rotation are the following:

2.2   Neuronal Network Training

We find candidate structures in the media and intima, which can follow the vessel wall kinematic during approximately a complete period of one cardiac event ≈ 25 images. In order to find the potential candidate structures, a Perceptron Multilayer Neural Network $(60 : 50 : 60 : 30)$ was trained using a standard Back Propagation Algorithm [9]. The input features were the radial grey level intensity defined as: $I(r) = I_o exp(-\alpha(N_\theta)rf)$, where I_o is the beam intensity at $r = 0$ and the absorbtion coefficient, α gives the rate of diminution of average power
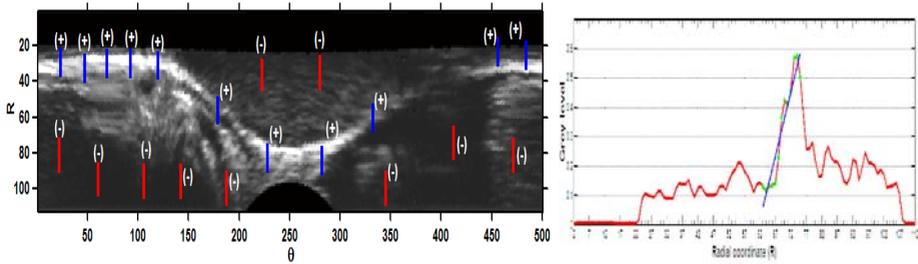
Fig. 2. Positive (+) and negative (-) pattern (left). Positive pattern features (right)
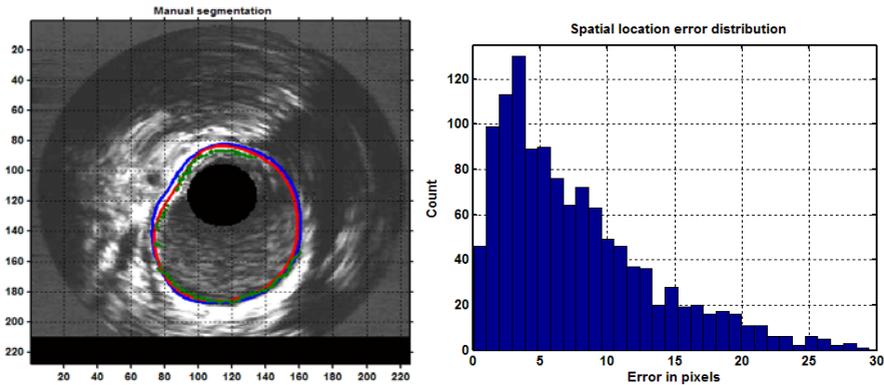
Fig. 3. Intima validated segmentation (left). Error distribution in mm (right)

with respect to the distance along a transmission path [7]. It is composed of two parts, one (absorption) proportional to the frequency f, the other (scattering) dependent on the ratio of grain, particle size or the scatterer number N_θ located along the ultrasound beam path. Absorption coefficient, image pixel grey level, standard deviation and mean of the data were used to train the Neural Network. The absorption coefficient gives local information about the lumen-vessel transition, the grey level distribution gives local and global information about the vessel structure. The global and local vessel wall structure information is given by the low and high frequencies, of the grey level distribution. Standard deviation gives global textural information and the mean of the data is the base line of the global grey level intensity. The training and test data were obtained from IVUS images in polar form. Figure 2 (left) shows an example of a positive (+) corresponding to intima and negative (-) patterns, corresponding to blood, adventitia, shadows and artifact zones. The extraction of features for positive patterns is show in Fig. 2 (right). The local absorption coefficient was obtained from the regression line slope [15] of the image profile, grey level intensity vs. radial penetration. Figure 3 (left) shows an example of the validated data and its error spatial location (center) computed by 4 IVUS sequences of different

patients. The error is defined as, the Euclidean distance between the manual location of intima and the spatial location found out by the Neural Network algorithm. In order to improve the rotation center, the spatial location of the selected points should be greater as the vessel wall border. Although the spatial error between validated intima points find out by the neuronal network is as high as 5 pixels $\mp$ 12 (See Fig. 3 (right)), nevertheless with the selected intima points recovery of temporal kinematics is optimal. This fact makes the method very flexible since the main goal of this work is to find the global kinematic of the vessel wall not the vessel segmentation. In this sense we find the global motion of the structure physically connected to the vessel (intima and media) border whose thickness is approximately 10 to 15 pixels. Figure 3 (right) shows an elliptical approximation and the intima point find out by the neuronal network.

2.3   The IVUS Image Rotation Estimation

a. **Center estimation.** We determine the spatial location of the rotation center (x_c, y_c) in frame k, as the position (ij) on the vessel wall that has a minimal total energy given by (Eq. 2.1). The spatial location of the rotation center is put into the image point that reaches the condition:

$$(x_c, y_c) = argmin_{ij} \sum_{k=1}^{f_n} E_{ij}^k$$

where $f_n = 25$ is the image number used to evaluate this condition and (ij) are the row and columns of the average IVUS images. Figure 4 shows the kinematics parameters used by the estimation of the total energy such as required in Eq. 2.1. The temporal evolution of the vessel wall candidates is obtained using their kinematics variables: radial coordinates (a) and angular position (b). The total energy is computed considering that all points having the same mass (See section 2.1). Figure 4 (c) shows the minimal energy distribution for a particular frame and 25 candidates. The spatial evolution of the center of rotation is shown in Fig. 4 (d).

b. **Angle estimation.** Once the rotation center of the IVUS sequence has been determined, the procedure to calculate the rotation angle for each frame is as follows: 1.- An elliptical approximation following the ellipse fitting procedures of [16] is adjusted to the spatial distribution of the points structures (See Fig. 5). The fitting of ellipses is made over the mean of the IVUS sequence in the longitudinal direction. If the ellipse center is noted by (x_e^k, y_e^k), then the rotation angle α_k (See Fig. 5) for a frame k is given by:

$$\alpha_k = \arctan \left(\frac{y_e^k - y_c^k}{x_e^k - x_c^k} \right)$$

where (x_e^k, y_e^k) and (x_c^k, y_c^k) are the rotation center and ellipse center of image k respectively.

(a)

(b)

(c)

(d)
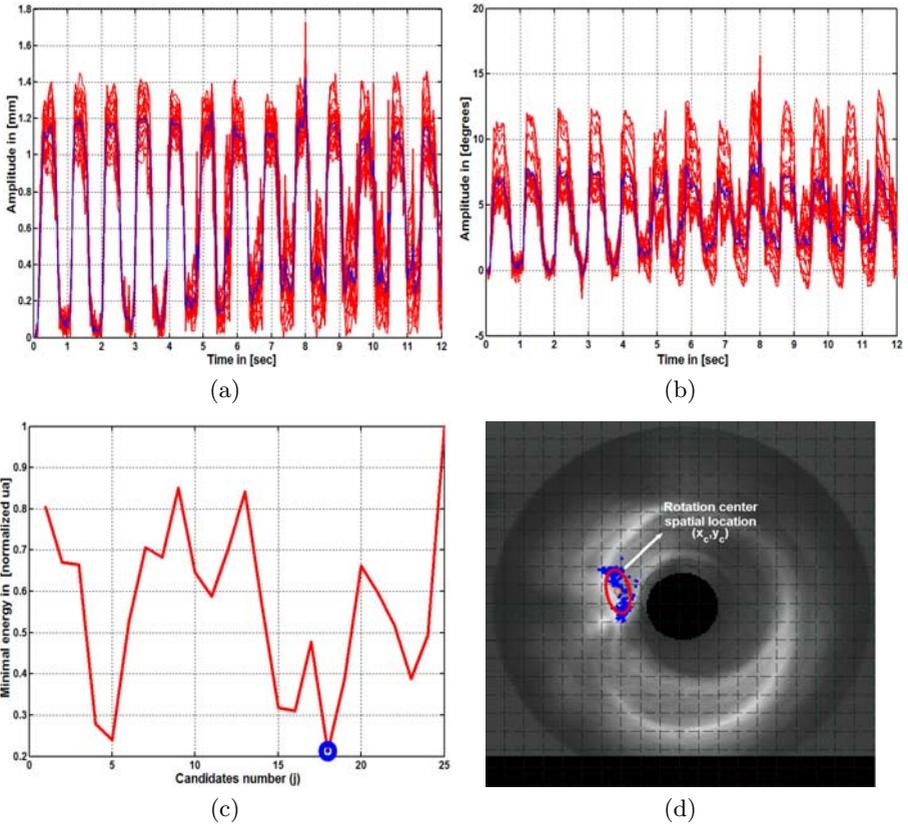
Fig. 4. Kinematics variables: r (a) and θ (b) coordinates evolution. Minimal energy (d) location by 25 candidates points. Rotation center location (d)
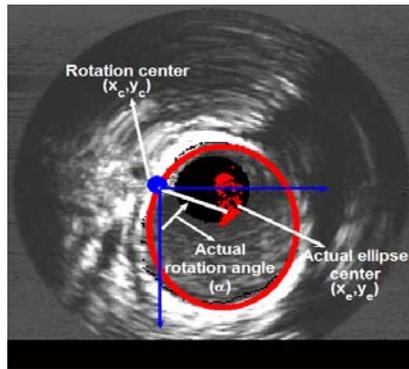
Fig. 5. Parameters to estimate the IVUS image rotation α_k

2.4   Removing the IVUS Rotation Effect

The suppression of the rotation is given by the following linear transformation: The original image $I_o(x, y)$ is translated to the rotation center coordinates (x_c^k, y_c^k) and rotated through angle α_k. The new image $I_o'(x', y')$ is finally located in a new arbitrary center (x_a^k, y_a^k) as follows:

$$\begin{pmatrix} x' \\ y' \end{pmatrix} = \begin{pmatrix} sin(\alpha_k) & cos(\alpha_k) \\ -cos(\alpha_k) & sin(\alpha_k) \end{pmatrix} \begin{pmatrix} x - x_c^k \\ y - y_c^k \end{pmatrix} + \begin{pmatrix} x_a^k \\ y_a^k \end{pmatrix} \qquad (2)$$

where (x', y') and (x, y) are the new and old cartesian image coordinates, (x_c^k, y_c^k) is the actual rotation center, α_k is the rotation angle and (x_a^k, y_a^k) is the new image center of image respectively.

3   Results

Our experiments focus on assessment of the rotation suppression and illustration of a possible application to pathology diagnosis.

3.1   Validation of the Rotation Suppression

Validation of rotation removing is done by analyzing the temporal evolution of the rotation angles. We consider that the rotation has been removed if the rotation angle profile after correction is constant to zero. There are several ways of checking the former hypothesis. First, we can compare the temporal evolution of the angle before and after rotation suppression. Lack of rotation is also reflected in average images and longitudinal cuts. After suppression there is no grey level shift so that bright structures stay still and the longitudinal cuts shape is a straight line in contrast to the wavy shape of original cuts. The former analysis is illustrated in Fig. 7. Rotation profiles before and after removing the rotation artifact are shown in Fig. 6 (a) and (b), respectively. In figure 7 (a) and (b) we depict the average sequences image with their corresponding centers of the adjusted ellipses. Note that their spatial variation has significantly reduced after image correction. Finally, longitudinal cuts before and after rotation elimination are exhibited in figure 7 (c) and (d).

3.2   Healthy and Pathological Rotations Profiles

We studied the local rotation profile in order to illustrate differences between healthy and pathological vessel segments. The comparative analysis is based on the period and the amplitude of the profile. For our basic comparative analysis we considered a healthy segment and 28 pathological ones including soft plaque, hard plaque and atheroma. Graphics along 250 frames are shown in Fig.8. The healthy patient presents a regular periodic behavior with an oscillation amplitude of approximately 40 degrees and a period that coincides with the heart beat rate.
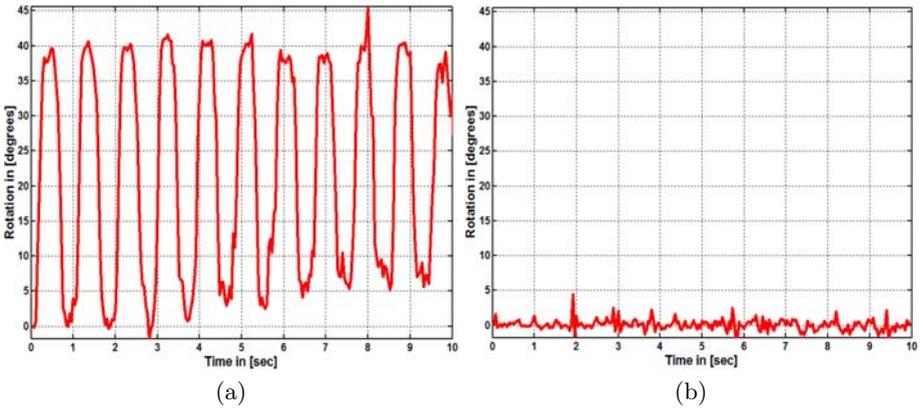
Fig. 6. Angle rotation profiles, before (a) and after (b) rotation suppression
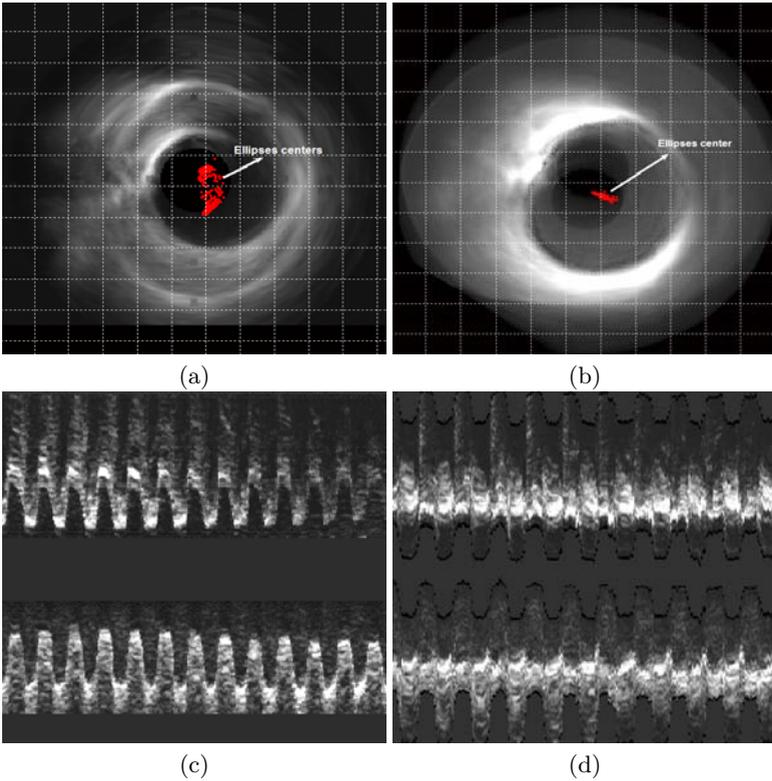
Fig. 7. Ellipses centers spatial location, before (a) and after (b) correction of rotation. Longitudinal cuts before(c) and after (d) rotation suppression
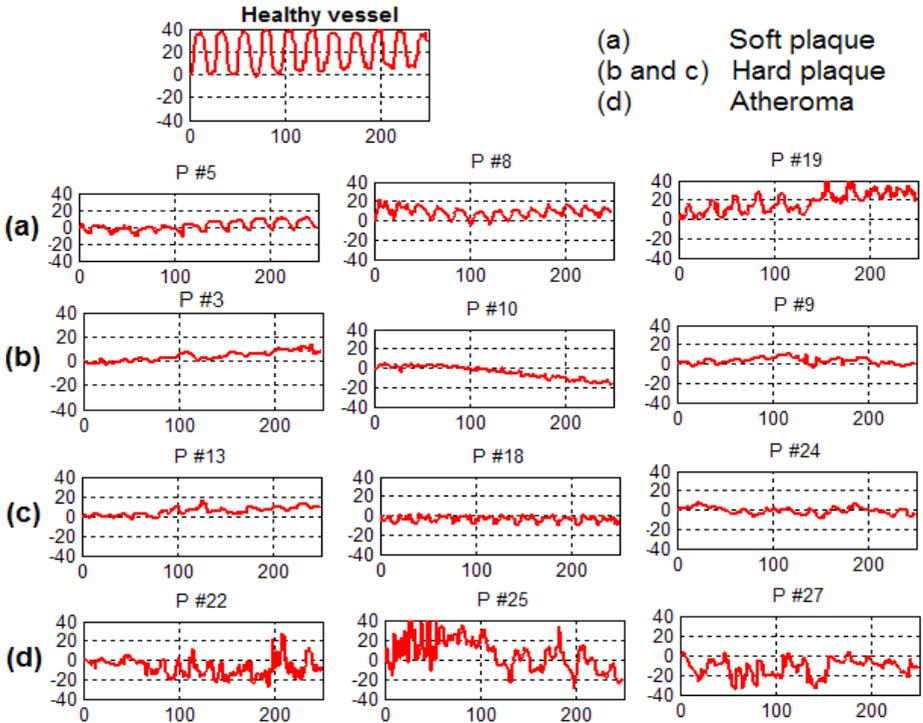
Fig. 8. Differences between healthy and pathological vessel segments of the rotation profiles for selected patients

Soft plaque still follows a periodic pattern synchronized with the heart beat, although its amplitude drops to a range of 5 to 20 degrees, depending on the severity of the lesion. The mechanical properties (elasticity and rigidity) of hard plaque result in a suppression of vessel oscillation, yielding almost flat rotation profiles. Finally, the atheroma profile is the most irregular one lacking of any visual periodicity.

4   Conclusions

The clinical applications of the rotation artifact have not been reported today, since the physiological, physical and geometrical reasons are not well known. We developed a kinematic model that allows to estimate and remove the IVUS rotation images effect. The model is based on the assumptions that the vessel wall shape can be modelled as a discrete structure. The proposed kinematic model can be used two ways: IVUS stabilization and kinematics characterization of the vessel wall. The first aspect is the main goal of this work, therefore we introduced a kinematics method to estimate and remove the rotation of IVUS sequences.

The method is based on the assumption that the vessel wall can be described as a discrete structure which kinematics temporal evolution can be followed by a trained Neural Network, during at least one heart cycle. A first examination of the qualitative shape of the rotation IVUS sequence profiles shows that the rotation effect can be used as a complementary tool, to evaluate vessel pathologies from kinematic point of view. Due to the anatomical distribution of the coronary arteries, most of the IVUS sequences ($> 85\%$), have their rotation center in the vessel wall border. Still some sequences have the rotation center located in the lumen center. In these cases in order to improve this first approach, a general geometric model based on the vessel wall kinematics must be considered. This is an object of our future work.

References

1. Yock P., Linker D., and et al., Intravascular two dimensional catheter ultrasound, Initial clinical studies, Circulations, No. 78, II-21, 1988.
2. Graham S., Brands D., and et al., Assesment of arterial wall morphology using intravascular ultrasound in vitro and in patient, Circulations, II-56, 1989.
3. Metz J., Paul G., and et al Intravascular Ultrasound Imaging, Jonathan M. Tobis y Paul G. Yock. Churchil Livinstone Inc., 1992.
4. Metz Jonas A., Paul G., and et al, Intravascular ultrasound basic interpretation, in Beyond Angiography, Intravascular Ultrasound, State of the art, Vol. XX, Congress of the ESC Viena-Austria, California, USA., 1998.
5. Jumbo G., Raimund E., Novel techniques of coronary artery imaging, in Beyond Angiography, Intra Vascular Ultrasound, state of the art, Vol. XX, Congress of the ESC Viena-Austria, University of Essen,Germany, 1998.
6. Di Mario C., et al. The angle of incidence of the ultrasonic beam a critical factor for the image quality in intravascular ultrasonography. Am Heart J 1993;125:442-448.
7. Arendt Jesen J., Linear Descripcion of Ultrasound Imaging System, Notes for the international Summer School on Advanced Ultrasound Imaging, Tecnical University of Denamark, 2001.
8. Berry E., and et al, Intravascular ultrasound-guided interventions in coronary artery disease, NHS R D HTA Programme, 2000.
9. Patrick H. W. Inteligencia Artificial, Addison Wesley Iberoamericana, 1994.
10. Korte Chris L., Intravascular Ultrasound Elastography, Interuniversity Cardiology Institute of the Netherlands (ICIN), 1999.
11. Mazumdar J., Biofluids Mechanics, World Scientific Publishing, 1992.
12. Young B., and Heath J., Wheater's, Histología Funcional, 4ta edición, Ediciones Hardcourt, S.A, 2000.
13. Boston Scientific Corporation, Scimed division, The ABCs of IVUS, 1998.
14. Misael Rosales, Petia Radeva and et al. Simulation Model of Intravascular Ultrasound Images, Lecture Notes in Computer Science Publisher: Springer-Verlag Heidelberg, Medical Image Computing and Computer-Assisted Intervention MICCAI 2004, Volume 3217/ 2004, pp. 200-207, France, September, 2004.
15. Vogt M., and et al, Strutural analysis of the skin using high frequency broadband ultrasound in the range from 30 to 140 mhz, IEEE Internationalk Ultrasonics Syposium, Sendai, Japan, 1998.
16. Andrew W. and et al, Direct Least Square Fitting of Ellipses, IEEE Transactions on Pattern Analysis and Machine Intelligence, vol 21, number 5, p 476-480, 1999